



PCT/GB2004/002966



INVESTOR IN PEOPLE

## PRIORITY DOCUMENT

SUBMITTED OR TRANSMITTED IN  
COMPLIANCE WITH RULE 17.1(a) OR (b)

REC'D 06 AUG 2004

WIPO PCT

The Patent Office  
Concept House  
Cardiff Road  
Newport  
South Wales  
NP10 8QQ

I, the undersigned, being an officer duly authorised in accordance with Section 74(1) and (4) of the Deregulation & Contracting Out Act 1994, to sign and issue certificates on behalf of the Comptroller-General, hereby certify that annexed hereto is a true copy of the documents as originally filed in connection with the patent application identified therein.

In accordance with the Patents (Companies Re-registration) Rules 1982, if a company named in this certificate and any accompanying documents has re-registered under the Companies Act 1980 with the same name as that with which it was registered immediately before re-registration save for the substitution as, or inclusion as, the last part of the name of the words "public limited company" or their equivalents in Welsh, references to the name of the company in this certificate and any accompanying documents shall be treated as references to the name with which it is so re-registered.

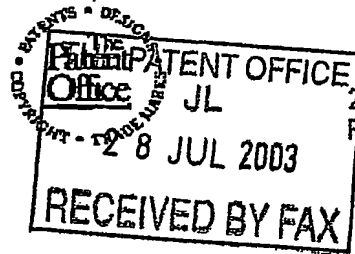
In accordance with the rules, the words "public limited company" may be replaced by p.l.c., plc, P.L.C. or PLC.

Re-registration under the Companies Act does not constitute a new legal entity but merely subjects the company to certain additional company law rules.

Signed

*Andrew Jersey*

Dated 22 July 2004

28JUL03 E825837-1 D02987  
F01/7700 0.00-0317600.5

The Patent Office

Cardiff Road  
Newport  
South Wales  
NP10 8QQ

## Request for grant of a patent

(See the notes on the back of this form. You can also get an explanatory leaflet from the Patent Office to help you fill in this form)

1. Your reference

2768

2. Patent application number

(The Patent Office will fill in this part)

0317600.5

28 JUL 2003

3. Full name, address and postcode of the or of each applicant (underline all surnames)

University of Southampton  
Highfield

Patents ADP number (if you know it)

Southampton  
SO17 1BJ 798470001  
UK4. Title of the invention Extending the Memory of Nuclear Spins:  
Singlet States in Low Magnetic Field

5. Name of your agent (if you have one)

Centre for Enterprise and Innovation  
(CEI)"Address for service" in the United Kingdom  
to which all correspondence should be sent  
(including the postcode)

University of Southampton

7989916001

Highfield

Southampton

SO17 1BJ, UK

Patents ADP number (if you know it)

6. If you are declaring priority from one or more earlier patent applications, give the country and the date of filing of the or of each of these earlier applications and (if you know it) the or each application number

Country

Priority application number  
(if you know it)Date of filing  
(day / month / year)

7. If this application is divided or otherwise derived from an earlier UK application, give the number and the filing date of the earlier application

Number of earlier application

Date of filing  
(day / month / year)

8. Is a statement of inventorship and of right to grant of a patent required in support of this request? (Answer 'Yes' if:

- any applicant named in part 3 is not an inventor; or
- there is an inventor who is not named as an applicant; or
- any named applicant is a corporate body.

See note (d))

No

Patents Form 1/77

9. Enter the number of sheets for any of the following items you are filing with this form.  
Do not count copies of the same document

Continuation sheets of this form

Description 15 ✓

Claim(s)

Abstract ✓

Drawing(s)

4 ✓

10. If you are also filing any of the following, state how many against each item.

Priority documents

Translations of priority documents

Statement of inventorship and right to grant of a patent (Patents Form 7/77)

Request for preliminary examination and search (Patents Form 9/77)

Request for substantive examination  
(Patents Form 10/77)

Any other documents ✓  
(please specify) Covering letter (1), 14.77-(2), Figure captions (3),  
Supporting material (7) = 13 ✓

11.

✓ We request the grant of a patent on the basis of this application.

Signature

Laura Keene

Date 28/7/03

12. Name and daytime telephone number of person to contact in the United Kingdom

Laura Keene 02380 591035

Warning

After an application for a patent has been filed, the Comptroller of the Patent Office will consider whether publication or communication of the invention should be prohibited or restricted under Section 22 of the Patents Act 1977. You will be informed if it is necessary to prohibit or restrict your invention in this way. Furthermore, if you live in the United Kingdom, Section 23 of the Patents Act 1977 stops you from applying for a patent abroad without first getting written permission from the Patent Office unless an application has been filed at least 6 weeks beforehand in the United Kingdom for a patent for the same invention and either no direction prohibiting publication or communication has been given, or any such direction has been revoked.

Notes

- a) If you need help to fill in this form or you have any questions, please contact the Patent Office on 08459 500505.
- b) Write your answers in capital letters using black ink or you may type them.
- c) If there is not enough space for all the relevant details on any part of this form, please continue on a separate sheet of paper and write "see continuation sheet" in the relevant part(s). Any continuation sheet should be attached to this form.
- d) If you have answered 'Yes' Patents Form 7/77 will need to be filed.
- e) Once you have filled in the form you must remember to sign and date it.
- f) For details of the fee and ways to pay please contact the Patent Office.

# **Extending the Memory of Nuclear Spins: Singlet States in Low Magnetic Field**

*One-Sentence Summary:* Low-field nuclear magnetic singlet states allow the storage of nuclear spin order for much longer than the conventional relaxation time limit.

(

## Abstract

Nuclear spin singlet states may be used to store nuclear spin order in a room temperature liquid for a time much longer than the spin-lattice relaxation time constant  $T_1$ . The nuclear spin singlets are unaffected by intramolecular dipole-dipole relaxation, which is generally the predominant relaxation mechanism. We demonstrate storage of nuclear spin order for more than ten times longer than the measured value of  $T_1$ . This phenomenon may facilitate the development of nuclear spin hyperpolarization methods, and may allow the study of motional processes which occur too slowly for existing NMR techniques.

One of the principal factors contributing to the wide-ranging utility of nuclear magnetic resonance (NMR) is the relatively long lifetime of nuclear spin order. This long lifetime allows NMR spectroscopists to follow processes such as diffusion, flow and slow molecular motion (1,2), and to contemplate using NMR for quantum computation (3,4). The relaxation of the nuclear spins back to thermal equilibrium, and hence the lifetime of the nuclear spin memory, is characterized by a time constant  $T_1$  known as the longitudinal relaxation time constant, or as the spin-lattice relaxation time constant. In most cases, this parameter is of the order of seconds, although it may be much longer in special cases. Major changes in  $T_1$  can usually only be achieved by changing the isotopic composition of the sample, or by changing its physical state. The sophisticated manipulation of nuclear spin interactions by radio-frequency pulse sequences, so prevalent in modern NMR (1), have always been restricted to a time-frame set by the intrinsic  $T_1$  limit. Experiments which seek to enhance NMR signals by hyperpolarization phenomena (5-9) have great potential for extending the range of NMR even further, but are always hampered by the need to use the hyperpolarized substance within a time of the order of  $T_1$ .

In this report, we demonstrate, for the first time, the storage of nuclear spin order for a time much longer than  $T_1$ . So far, we have demonstrated

this phenomenon on molecules containing pairs of protons, in which the main mechanism for nuclear spin relaxation is the modulation of the intramolecular dipole-dipole coupling by molecular motion. The extension of nuclear spin memory beyond the  $T_1$  limit is achieved by creating nuclear spin singlet states in low magnetic field (20 mT or less). As shown below, these low-field singlet states (LFS) are immune to the dominant intramolecular dipole-dipole mechanism and hence relax with a time constant much longer than the conventional  $T_1$ . The LFS states are generated by adiabatic transfer from non-equilibrium high-field states. The singlet states are allowed to decay in low field, and then transferred adiabatically back to high field where they can be detected as perturbations of conventional NMR signals. Low-field singlet states have been observed to decay with a time constant  $T_{\text{LFS}} = 104 \pm 5$  s, in a sample for which the measured  $T_1$  is  $16.8 \pm 0.3$  s under identical conditions.

The experimental procedure for investigating the lifetime of low-field singlet states is sketched in Fig.1. In its simplest form, the experiment applies to an ensemble of molecules, each containing a pair of spins-1/2 of the same isotopic type, but with different chemical shifts  $\delta_1$  and  $\delta_2$ , and a mutual J-coupling  $J$ . The experimental procedure uses a physical transport of the sample between two different magnetic field strengths,  $B_{\text{high}}$  and  $B_{\text{low}}$ , where  $B_{\text{high}} \gg B_{\text{low}}$ , as shown in Fig.1a. The transport processes from high to low field, and vice versa, take times  $\tau_{\text{transp}}^{(1)}$  and  $\tau_{\text{transp}}^{(2)}$  respectively, which are assumed to be less than  $T_1$  (both intervals are of the order of 10 seconds)

Fig.1

in the experiments reported here). The low-field storage interval  $\tau_{LF}$ , on the other hand, may be much longer than  $T_1$ . The transport between the two magnetic fields is synchronized with two radiofrequency pulse sequences denoted  $A_+$  and  $B$  in Fig.1b. These pulse sequences are applied at the Larmor frequency of the spins in the high magnetic field, and are specified in *Supporting Material*.

The energy level picture at time point ① in Fig.1c shows the four Zeeman energy levels, with energies in the order  $E_{\alpha\alpha} < E_{\alpha\beta} < E_{\beta\alpha} < E_{\beta\beta}$ , assuming that  $\delta_2 > \delta_1$ , the gyromagnetic ratio  $\gamma$  and the  $J$ -coupling are both positive, and that the spin system is weakly-coupled in high field. In thermal equilibrium at ambient temperature, the lowermost level  $|\alpha\alpha\rangle$  has a small excess population (depicted by the filled balls), while the uppermost level  $|\beta\beta\rangle$  has a slightly depleted population (depicted by the white balls). These population differences are very small in the case of conventional thermal polarization, but may be of the order of one in spin hyperpolarization experiments (5-9).

As discussed in *Supporting Material*, the pulse sequence  $A_+$ , which is given by two  $90^\circ$  pulses separated by a delay, exchanges the population of state  $|\alpha\alpha\rangle$  with that of  $|\alpha\beta\rangle$ , and that of  $|\beta\alpha\rangle$  with that of  $|\beta\beta\rangle$ . Hence, at time point 2, a non-equilibrium population distribution is generated, in which level  $|\alpha\beta\rangle$  has an excess population, while  $|\beta\alpha\rangle$  has a depleted population, as shown for time point ② in Fig.1c.

During the interval  $\tau_{\text{transp}}^{(1)}$ , the sample is transported to a region of low magnetic field  $B_{\text{low}}$ , which is of the order of milliTesla. In low field, it is convenient to discuss the behaviour of the nuclear spins using the four eigenstates of the pure  $J$ -coupling Hamiltonian:

$$\mathcal{H}_J = 2\pi J I_1 \cdot I_2 \quad [1]$$

The four  $J$ -coupling eigenstates may be classified as the three components of a triplet state, plus a singlet state. The triplet state components are denoted

$$\begin{aligned} |T_1\rangle &= |\alpha\alpha\rangle \\ |T_0\rangle &= \frac{1}{\sqrt{2}}(|\alpha\beta\rangle + |\beta\alpha\rangle) \\ |T_{-1}\rangle &= |\beta\beta\rangle \end{aligned} \quad [2]$$

and have the same  $J$ -coupling eigenvalue of  $+\frac{1}{2}\pi J$ . The singlet state is denoted

$$|S_0\rangle = \frac{1}{\sqrt{2}}(|\alpha\beta\rangle - |\beta\alpha\rangle) \quad [3]$$

and has a  $J$ -coupling eigenvalue of  $-\frac{3}{2}\pi J$ . The triplet and singlet states are energy eigenstates of the nuclear spins only if the magnetic field is zero. The energy level diagram in this case is depicted next to time point ③ in Fig.1c. Although we use the zero-field eigenstates as a basis for a representation of

the spin density operator, the treatment below does not assume a field of exactly zero.

If the transport from high to low field is fast compared to  $T_1$ , but slow compared to the  $J$ -coupling, the excess population of the high-field eigenstate  $|\alpha\beta\rangle$  is transferred adiabatically into an excess population of the low-field eigenstate  $|S_0\rangle$ . Similarly, the depleted population of the high-field eigenstate  $|\beta\alpha\rangle$  is transferred adiabatically into a depleted population of the zero-field eigenstate  $|T_0\rangle$ . These adiabatic transfer processes have been exploited before in the context of parahydrogen-enhanced NMR (7). The idealized distribution of the singlet and triplet state populations is shown at time point ③ in Fig.1c. This assumes pure adiabatic transfer and neglects  $T_1$  relaxation during the transport interval.

The nuclear spins evolve in low magnetic field under a combination of coherent effects and incoherent relaxation processes. The coherent part of the low-field evolution has been studied before (10,11) but the analysis of incoherent molecular motion in very low field NMR has been restricted to the motional averaging of interaction tensors and to the investigation of lineshape perturbations (12-15). Here we use a standard second-order perturbation treatment of the modulated dipole-dipole interaction (16) to analyze the spin-lattice relaxation in low field.

In general, the spin density operator  $\rho$  evolves according to the Liouville-von Neumann equation (1)

$$\frac{d}{dt}\rho(t) = \hat{\tilde{L}}_{LF}\rho(t) \quad [4]$$

where the low-field Liouvillian is given by

$$\hat{\tilde{L}}_{LF} = \hat{\tilde{\Gamma}}_{LF} - i\hat{\tilde{\mathcal{H}}}_{LF} \quad [5]$$

and  $\hat{\tilde{\mathcal{H}}}_{LF}$  is the superoperator for the commutator with the low-field spin Hamiltonian:

$$\mathcal{H}_{LF} = -\gamma B_{low}(1 + \delta_1)I_{1z} - \gamma B_{low}(1 + \delta_2)I_{2z} + \mathcal{H}_J \quad [6]$$

The thermal polarization terms (17) may be ignored in low field. If the relaxation is dominated by the intramolecular dipole-dipole coupling mechanism, the relaxation superoperator may be evaluated by second-order time-dependent perturbation theory and is given by (1)

$$\hat{\tilde{\Gamma}}_{LF} \cong - \int_{-\infty}^0 \overline{\hat{\tilde{\mathcal{H}}}_{DD}(-\tau)\hat{\tilde{\mathcal{H}}}_{DD}(0)} d\tau \quad [7]$$

where  $\hat{\tilde{\mathcal{H}}}_{DD}(t)$  is the commutation superoperator for the dipole-dipole coupling Hamiltonian, evaluated at time  $t$ , and the overbar represents an ensemble average. Eq.[4] is general for any field strength low enough to satisfy the extreme narrowing condition for the dipole-dipole relaxation.

It is convenient to use the matrix representation of the Liouvillian superoperator  $\hat{L}_{LF}$  in a space of orthonormal spin operators (18). The following set of six operators generate a suitable basis:

$$\begin{aligned}
 |1\rangle &= |S_0\rangle\langle S_0| &= \frac{1}{2}(I_1^\alpha I_2^\beta + I_1^\beta I_2^\alpha - I_1^+ I_2^- - I_1^- I_2^+) \\
 |2\rangle &= |T_1\rangle\langle T_1| &= I_1^\alpha I_2^\alpha \\
 |3\rangle &= |T_0\rangle\langle T_0| &= \frac{1}{2}(I_1^\alpha I_2^\beta + I_1^\beta I_2^\alpha + I_1^+ I_2^- + I_1^- I_2^+) \\
 |4\rangle &= |T_{-1}\rangle\langle T_{-1}| &= I_1^\beta I_2^\beta \\
 |5\rangle &= \frac{1}{2}(|S_0\rangle\langle T_0| + |T_0\rangle\langle S_0|) &= \frac{1}{\sqrt{2}}(I_1^\alpha I_2^\beta - I_1^\beta I_2^\alpha) \\
 |6\rangle &= \frac{1}{2i}(|S_0\rangle\langle T_0| - |T_0\rangle\langle S_0|) &= -i\frac{1}{\sqrt{2}}(I_1^+ I_2^- - I_1^- I_2^+)
 \end{aligned}$$

where  $I_j^\pm$  are single-spin shift operators and  $\{I_j^\alpha, I_j^\beta\}$  are single-spin polarization operators (1,2). The ket  $|1\rangle$  describes the population operators of the singlet state. Kets  $|2\rangle$ ,  $|3\rangle$  and  $|4\rangle$  describe the population operators of the three triplet states. Kets  $|5\rangle$  and  $|6\rangle$  represent the  $x$  and  $y$ -components of the coherence between the singlet state and the central component of the triplet. All of these operators commute with the angular momentum operator along the field axis, as does the low-field Hamiltonian  $H_{LF}$ . The operator basis in Eq.[8] is closed under the application of the low-field Liouvillian  $\hat{L}_{LF}$ .

The matrix representation of the low-field relaxation superoperator  $\hat{\Gamma}_{LF}$  may be evaluated by standard relaxation theory (1), assuming pure intramolecular dipole-dipole relaxation driven by rigid isotropic random rotation with

a correlation time  $\tau_c$ . The low-field Liouvillian evaluates to

$$\hat{L}_{LF} = \begin{pmatrix} 0 & 0 & 0 & 0 & 0 & -2^{-1/2}\omega_{\Delta}^{\text{low}} \\ 0 & -\frac{9}{10}b^2\tau_c & \frac{3}{10}b^2\tau_c & \frac{3}{5}b^2\tau_c & 0 & 0 \\ 0 & \frac{3}{10}b^2\tau_c & -\frac{3}{5}b^2\tau_c & \frac{3}{10}b^2\tau_c & 0 & 2^{-1/2}\omega_{\Delta}^{\text{low}} \\ 0 & \frac{3}{5}b^2\tau_c & \frac{3}{10}b^2\tau_c & -\frac{9}{10}b^2\tau_c & 0 & 0 \\ 0 & 0 & 0 & 0 & -\frac{1}{2}b^2\tau_c & 2\pi J \\ 2^{-1/2}\omega_{\Delta}^{\text{low}} & 0 & -2^{-1/2}\omega_{\Delta}^{\text{low}} & 0 & -2\pi J & -\frac{1}{2}b^2\tau_c \end{pmatrix}$$

[8]

where the dipole-dipole coupling between the spins is given by  $b = -(\mu_0/4\pi)\gamma^2\hbar r^{-3}$ , and  $r$  is the internuclear distance. The low-field chemical shift frequency difference is defined

$$\omega_{\Delta}^{\text{low}} = -\gamma B_{\text{low}}(\delta_2 - \delta_1) \quad [9]$$

In zero field ( $\omega_{\Delta}^{\text{low}} = 0$ ), the first row and column of Eq.[8] contain only zeros. This indicates that the singlet state population is dynamically isolated in low field, and is conserved under the evolution process. The zero-field singlet state may be used as a long-term repository for nuclear spin order, protected from intramolecular dipole-dipole relaxation.

If the magnetic field is not exactly zero, Eq.[8] indicates that the singlet state is relaxed indirectly by dynamic couplings to the central triplet state and to singlet-triplet coherence.

The idealized behaviour of the spin ensemble after an interval  $\tau_{LF}$  in low field is depicted by the diagram at time point ④ in Fig.1c. If the field is sufficiently low, and  $\tau_{LF}$  is long enough, the triplet populations equilibrate, while the singlet population is conserved.

The singlet population may be read out by adiabatic transport of the sample back into high field during the interval  $\tau_{transp}^{(2)}$ . This transforms the low-field singlet population into a population of the high-field  $|\alpha\beta\rangle$  state, as depicted for time point ⑤ in Fig.1c. The population of the  $|\alpha\beta\rangle$  state is converted into observable NMR signals by the pulse sequence *B*. As described in *Supporting Material*, this sequence, which is given by three rf pulses separated by two unequal delays, converts the  $|\alpha\beta\rangle$  state population into antiphase NMR signals centred at the chemical shift  $\delta_2$ . NMR signals deriving from  $T_1$  relaxation during the transport interval, on the other hand, only generate NMR signals at the chemical shift  $\delta_1$ . The interesting NMR signals deriving from low-field singlet storage are therefore cleanly separated from signals with a trivial origin.

Experimental results for a 17.7 mM solution of 2,3-dibromothiophene in DMSO-d<sup>6</sup> at 20°C are shown in Fig.2. The proton spin system is defined by  $\delta_1 = 7.11$  ppm,  $\delta_2 = 7.72$  ppm and  $J = 5.7$  Hz. A conventional proton NMR spectrum, obtained at 400 MHz in the field  $B_{high} \cong 9.4$  T, is shown in Fig.2a and displays the two doublets of a typical AX spin system. A conventional inversion-recovery series (not shown), shows that the spin-lattice

Fig.2

relaxation time constants for the inequivalent sites are very similar in high field ( $T_1(\delta_1) = 16.5 \pm 0.2$  s;  $T_1(\delta_2) = 17.1 \pm 0.2$  s).

Fig.2b shows the spectrum obtained after the singlet-storage sequence in Fig.1, using a storage time  $\tau_{LF} = 100$  s, and a storage field  $B_{low} = 1.8 \pm 0.5$  mT. The spectrum in Fig.2b shows diagnostic antiphase signals at around  $\delta_2 = 7.72$  ppm, and an antiphase dispersion structure around  $\delta_1 = 7.11$  ppm.

We can prove the phenomenon of low-field singlet storage by replacing the sequence  $A_+$  by the sequence  $A_-$ . As discussed in *Supporting Material*, the sequence  $A_-$ , which is derived from  $A_+$  by changing one of the pulse phases, exchanges the population of state  $|\alpha\beta\rangle$  with that of  $|\beta\beta\rangle$ , instead of with  $|\alpha\alpha\rangle$ . The population of  $|\alpha\beta\rangle$  is therefore depleted at time point ② rather than enhanced. Fig.2c shows the expected change in sign of the diagnostic antiphase signals around  $\delta_2 = 7.72$  ppm. The signals around  $\delta_1 = 7.11$  ppm are also perturbed, but in a more complicated way, since these signals are superpositions of several contributions (see *Supporting Material*). Since the total interval  $\tau_{transp}^{(1)} + \tau_{LF} + \tau_{transp}^{(2)} = 120$  s exceeds  $T_1$  by a factor of seven, the spectra in Fig.2b and c prove that the memory of the nuclear spin system has been extended significantly beyond the  $T_1$  limit.

Fig.3

Fig.3 shows the measured decay of the singlet population in low field, derived by monitoring the 7.72 ppm antiphase signals as a function of  $\tau_{LF}$ . In a field  $B_{low} = 1.8 \pm 0.5$  mT, the time constant for the singlet decay is estimated to be  $T_{LFs} = 104 \pm 5$  s. The singlet decay time constant had

no appreciable field-dependence for magnetic fields less than  $B_{\text{low}} = 20$  mT. This behaviour is expected from numerical calculations based on Eq. [8] (see *Supporting Material*).

The singlet decay is observed to accelerate when the proton concentration in the solution is increased. This indicates that intermolecular proton-proton relaxation is a strong contributor to the singlet relaxation, and that very long lifetimes may only be achievable in highly dilute solutions. Singlet relaxation is also expected to be caused by paramagnetic impurities such as dissolved oxygen, intermolecular interactions with solvent deuterons, and scalar relaxation of the second kind (16) via the Br nuclei.

The long-term persistence of the zero-field singlet state cannot be attributed to the field-dependence of  $T_1$ , which is very mild for the sample studied here. A more correct interpretation is that the low external field suppresses the chemical shift difference and renders the spins magnetically-equivalent, which isolates the singlet state from the triplet manifold, even with respect to dipole-dipole relaxation. In effect, the singlet nuclear spin state of 2,3-dibromothiophene is an analogue of parahydrogen, which is also a nuclear spin singlet (6-8).

The storage effect should be observable in systems of larger numbers of spins as long as magnetic equivalence can be switched on and off by a change in the external magnetic field strength. We are currently exploring four-proton systems of the form X-CH<sub>2</sub>-CH<sub>2</sub>-Y which should display a similar property.

Singlet storage effects should be observable entirely in high magnetic field if a suitable radiofrequency pulse sequence is used to suppress chemical shift differences (19). Analogous "zero-field experiments in high field" have been performed in solid-state NMR (20,21). Radiofrequency pulse sequences might be designed which allow the storage of nuclear spin order for times much longer than  $T_1$ , without removing the sample from the high-field magnet.

Extension of the spin memory time should be useful whenever nuclear spin states are used as a long-term label for the position or chemical state of molecules. The long lifetime of low-field singlet states is expected to facilitate nuclear hyperpolarization experiments, especially those involving parahydrogen (5-8), and may create new possibilities in the exploitation of NMR for quantum computation (3,4).

## References.

1. R. R. Ernst, G. Bodenhausen, A. Wokaun, *Principles of Nuclear Magnetic Resonance in One and Two Dimensions* (Clarendon Press, Oxford, UK, 1987).
2. M. H. Levitt, *Spin Dynamics. Basics of Nuclear Magnetic Resonance* (Wiley, Chichester, UK, 2001).
3. N. A. Gershenfeld, I. L. Chuang, *Science* 275, 350 (1997).
4. D. G. Cory, A. F. Fahmy, T. F. Havel, *Proc. Natl. Acad. Sci. USA* 94, 1634 (1997).
5. G. Navon *et al.*, *Science* 271, 1848 (1996).
6. C. R. Bowers, D. P. Weitekamp, *J. Am. Chem. Soc.* 109, 5541 (1987).
7. M. G. Pravica, D. P. Weitekamp, *Chem. Phys. Lett.* 145, 255 (1988).
8. K. Golman *et al.*, *Magn. Reson. in Medicine* 46, 1 (2001).
9. D. A. Hall *et al.*, *Science* 276, 930 (1997).
10. D. B. Zax, A. Bielecki, K. W. Zilm, A. Pines, *Chem. Phys. Lett.* 106, 550 (1984).
11. R. McDermott *et al.*, *Science* 295, 2247 (2002).
12. J. M. Millar, A. M. Thayer, D. B. Zax, A. Pines, *J. Am. Chem. Soc.* 108, 5113 (1986).
13. P. Meier, G. Kothe, P. Jonsen, M. Trecoske, A. Pines, *J. Chem. Phys.* 87, 6867 (1987).

14. T. P. Jarvie, A. M. Thayer, J. M. Millar, A. Pines,  
*J. Phys. Chem.* **91**, 2240 (1987).
15. P. Meier, G. Kothe, P. Jonsen, M. Trecoske, A. Pines,  
*J. Chem. Phys.* **87**, 6867 (1987).
16. A. Abragam, *The Principles of Nuclear Magnetism*  
(Clarendon Press, Oxford, 1961).
17. M. H. Levitt, L. Di Bari,  
*Phys. Rev. Lett.* **69**, 3124 (1992).
18. J. Jeener, *Adv. Magn. Reson.* **10**, 1 (1982).
19. J. D. Ellett, J. S. Waugh,  
*J. Chem. Phys.* **51**, 2851 (1969).
20. R. Tycko, *Phys. Rev. Lett.* **60**, 2734 (1988).
21. R. Tycko, *J. Chem. Phys.* **92**, 5776 (1990).

## Figure Captions.

**Fig.1.** (a) Sequence of magnetic fields used in the experiment. The sample is transported from a region of high magnetic field  $B_{\text{high}}$  into a region of low magnetic field  $B_{\text{low}}$  in a time  $\tau_{\text{transp}}^{(1)}$ . After remaining in the low field for a time  $\tau_{\text{LF}}$ , the sample is transported back into the high-field region, a process which takes a time  $\tau_{\text{transp}}^{(2)}$ .

(b) Radio-frequency pulse sequence performed at the Larmor frequency of the spins in high field. The pulse sequences  $A_+$  and  $B$  are specified in *Supplementary Material*.

(c) Idealized sequence of spin state populations during the experiment. The four high-field energy levels belong to the states  $|\beta\beta\rangle$ ,  $|\alpha\beta\rangle$ ,  $|\alpha\alpha\rangle$  and  $|\beta\alpha\rangle$ , reading in a clockwise direction starting with the upper state.

Fig.2. (a) Conventional  $^1\text{H}$  NMR spectrum of the solution of 2,3-dibromothiophene (inset) in  $\text{DMSO-d}_6$ .  
(b) Spectrum generated by the sequence in Fig.1, using the preparation sequence  $A_+$ , and a storage time  $\tau_{\text{LF}} = 100\text{ s}$ .  
(c) Spectrum generated by the sequence in Fig.1, using the preparation sequence  $A_-$  and a storage time  $\tau_{\text{LF}} = 100\text{ s}$ .  
Expanded sections of the spectra from 7.76 to 7.68 ppm are shown for (b) and (c). All spectra were obtained from a single signal acquisition. The spectra in (b) and (c) are expanded vertically by a factor of 2 compared to (a).

Fig.3. Decay of the diagnostic antiphase signals as a function of time  $\tau_{\text{LF}}$ . The top and lower half indicate the integrated amplitudes of the two components of the antiphase multiplet centred at 7.72 ppm. The symbols represent measurements at different storage fields  $B_{\text{low}}$ . The vertical scale represents the integrated amplitude of the spectral peaks as a percentage of their amplitude in an ordinary one-pulse NMR experiment. The solid lines are fits to decaying exponential functions with time constant  $T_{\text{LFg}} = 104\text{ s}$ . The singlet decay is independent of the storage field in this regime.

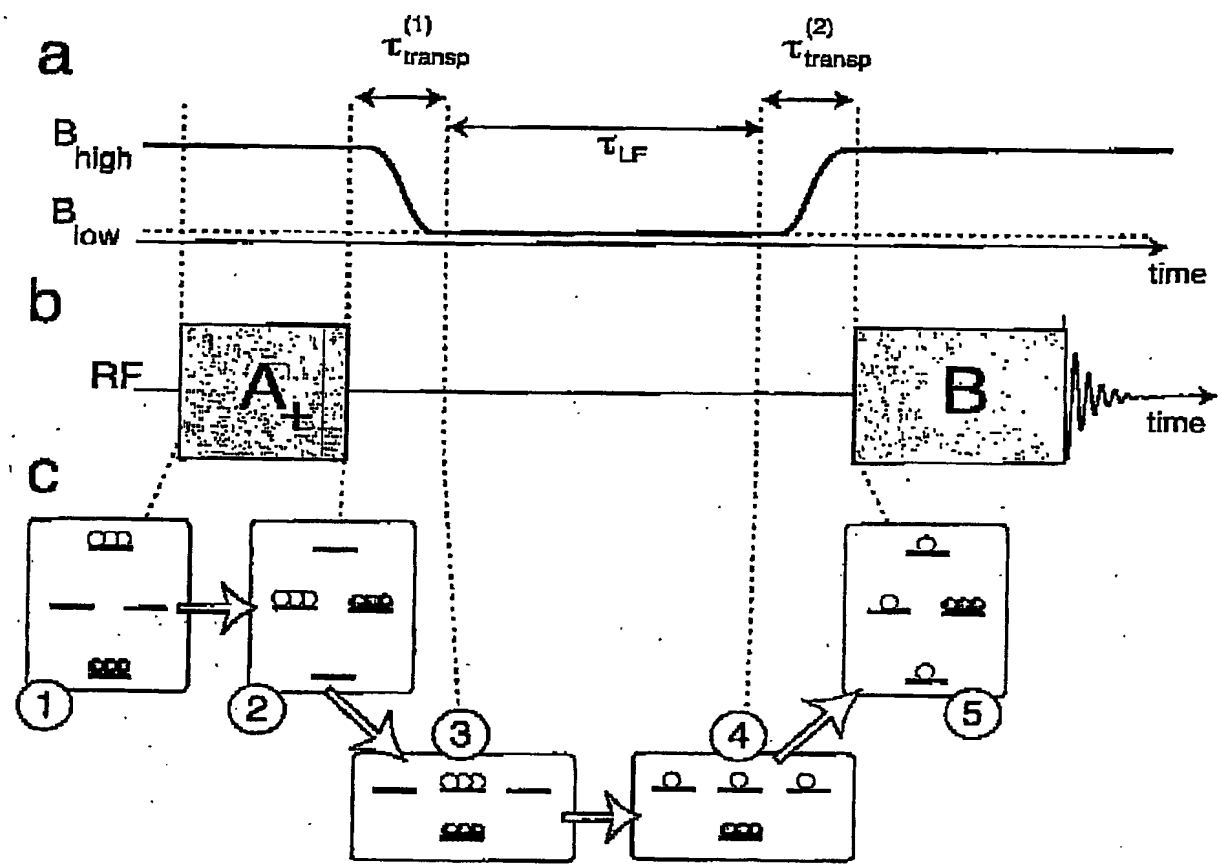


Fig.1

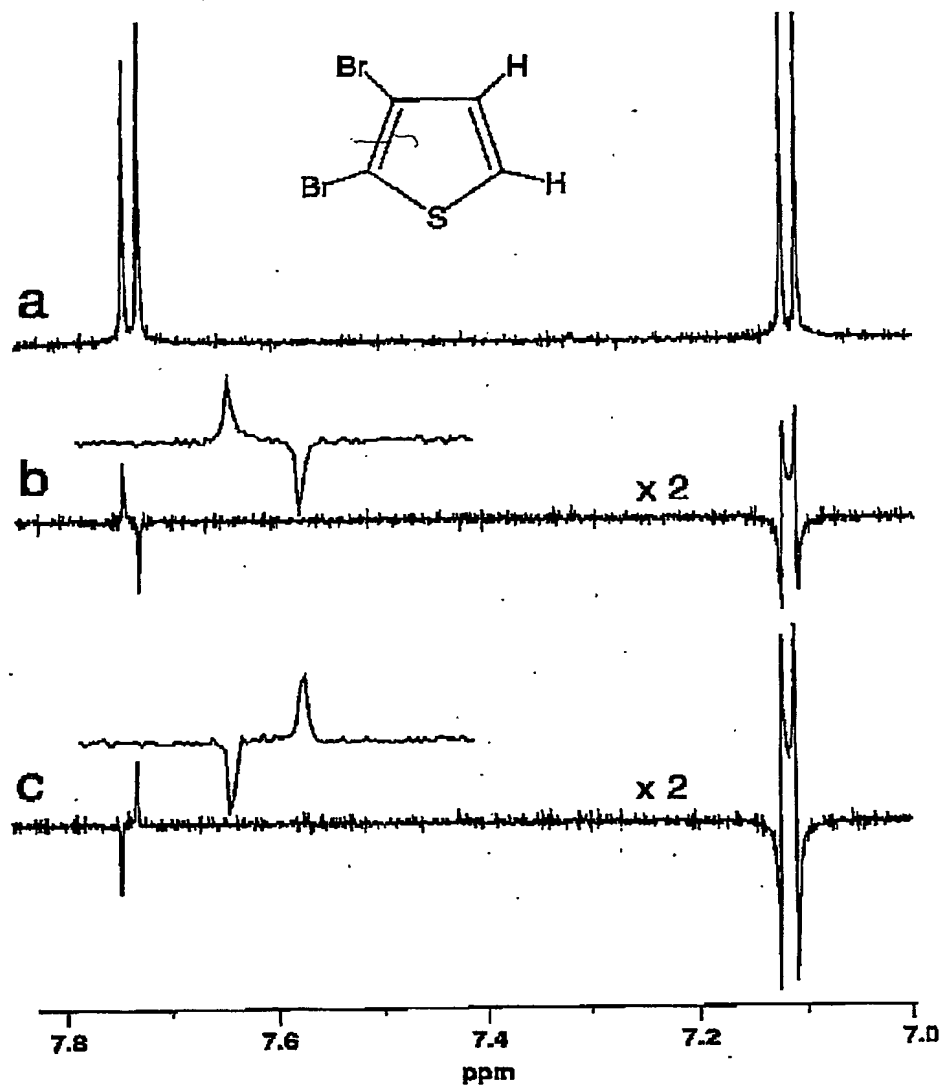


Fig.2

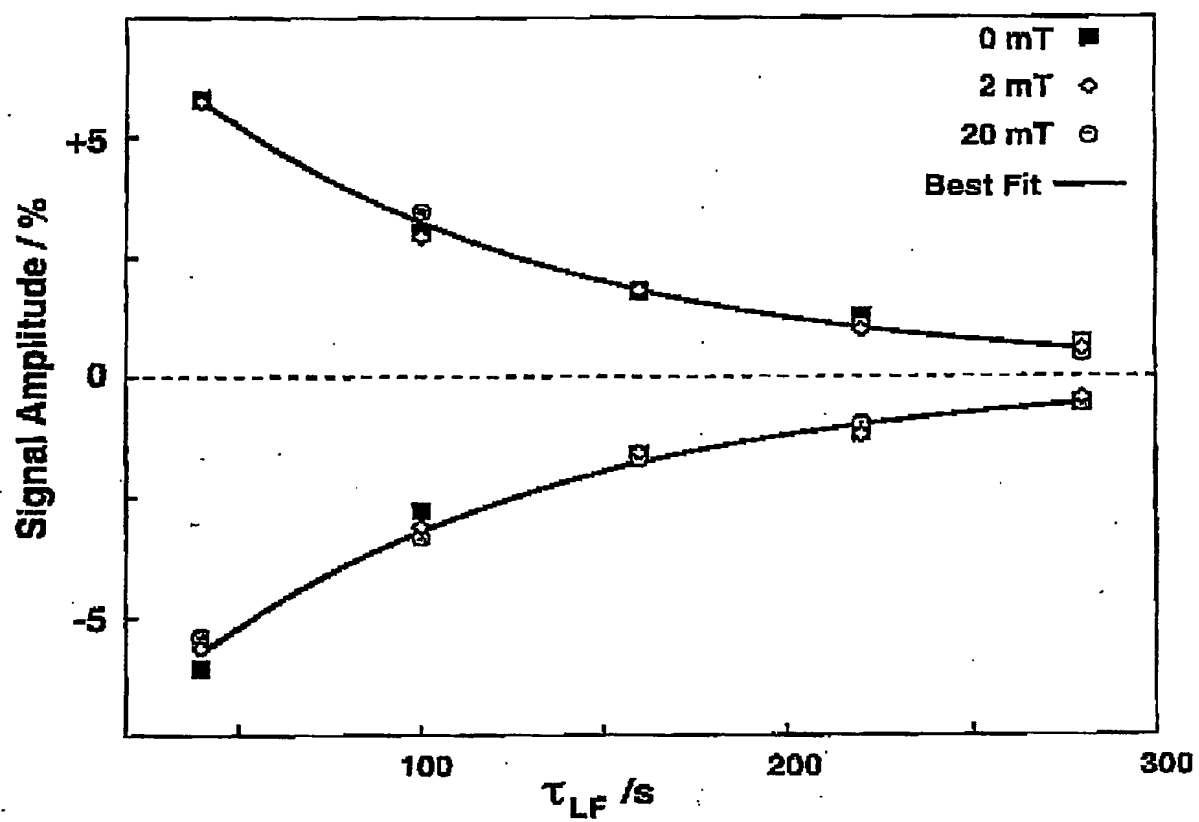
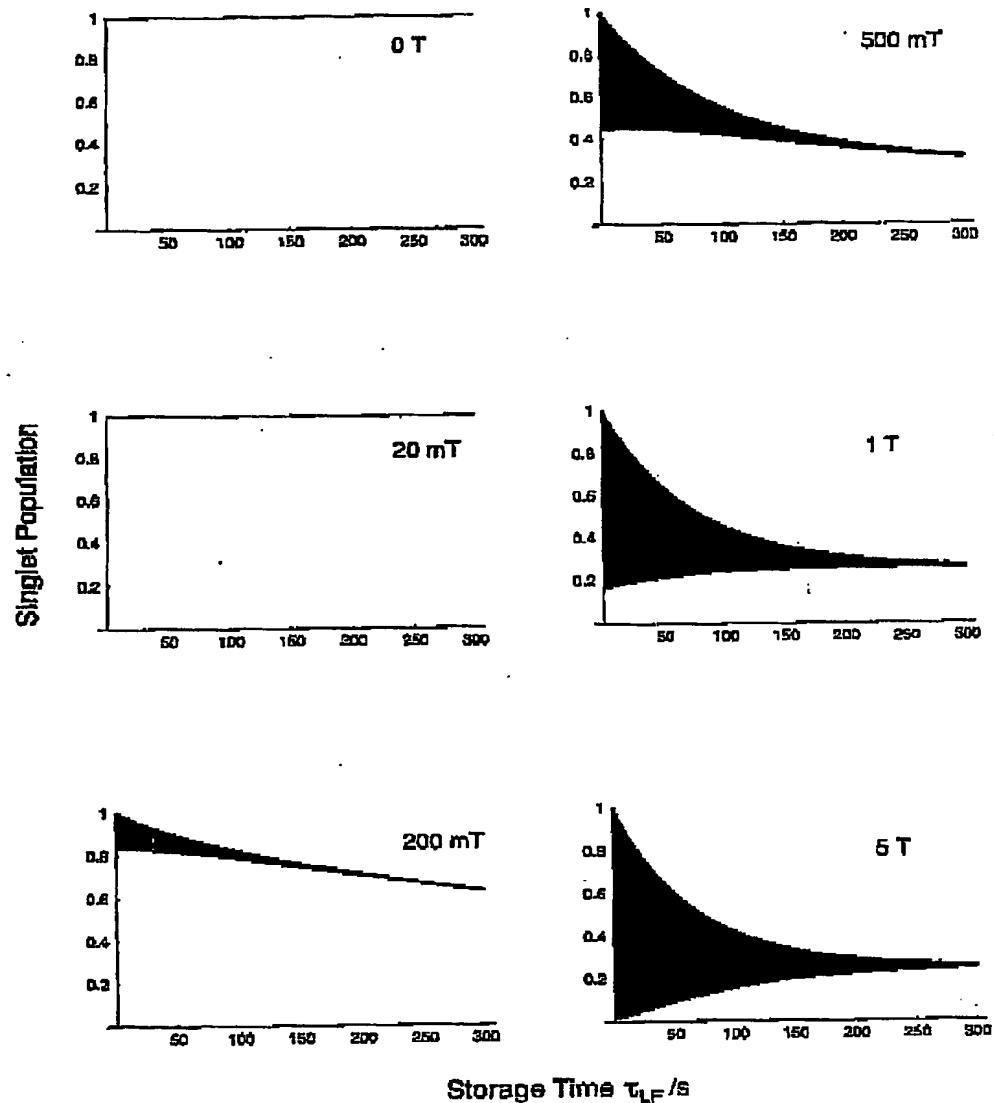


Fig.3



Supporting Material Fig.1

## Supporting Material

### Radiofrequency Pulse Sequences

#### Sequence $A_+$

The pulse sequence  $A_+$  is given by the two-pulse sequence  $90_\phi - \tau_1 - 90_{-\phi}$ , where the symbol  $90_\phi$  denotes a strong, non-selective pulse with flip angle  $\phi$  and phase  $\phi$  (both angles are specified in degrees, and the phases taken into account the sign of the precession and the radio-frequency mixing scheme (1,2)). The delay  $\tau_1$  is set to the value  $\tau_1 = |\pi/\omega_\Delta^{\text{high}}|$ , where

$$\omega_\Delta^{\text{high}} = -\gamma B_{\text{high}}(\delta_2 - \delta_1) \quad [1]$$

For the experimental results, the delay was set to the value  $\tau_1 = 2.05 \text{ ms}$ .

Standard spin operator theory (3,4) shows that in the case  $\delta_2 > \delta_1$  and  $\gamma > 0$ , the pulse sequence  $A_+$  has the approximate propagator

$$U(A_+) = \exp\{-i\frac{\pi}{2}(I_{1x} + I_{2z})\} \exp\{+i\pi I_{2y}\} \quad [2]$$

neglecting the effect of the  $J$ -coupling during the interval  $\tau_1$ . This assumption is valid in the case that the chemical shift frequency difference is much larger than the  $J$ -coupling (weak coupling approximation). The transformations of

the individual state kets are

$$U(A_+)|\alpha\alpha\rangle = -|\alpha\beta\rangle$$

$$U(A_+)|\beta\alpha\rangle = -i|\alpha\alpha\rangle$$

$$U(A_+)|\alpha\beta\rangle = -i|\beta\beta\rangle$$

$$U(A_+)|\beta\beta\rangle = |\beta\alpha\rangle \quad [3]$$

which leads to the exchanges of populations sketched in Fig. 1c. The population of the  $|\alpha\beta\rangle$  state at time point ② is derived from the thermal equilibrium population of the  $|\alpha\alpha\rangle$  state.

#### Sequence $A_-$

The pulse sequence  $A_-$  is given by the two-pulse sequence  $90_{180} - \tau_1 - 90_{-90}$ . The sequence differs from  $A_+$  by a  $180^\circ$  phase shift of the first pulse. The spin propagator for this sequence, under the weak-coupling approximation, is

$$U(A_-) = \exp\left\{+i\frac{\pi}{2}(I_{1x} + I_{2x})\right\} \exp\left\{+i\pi I_{1y}\right\} \quad [4]$$

which leads to the following ket transformations:

$$U(A_-)|\alpha\alpha\rangle = -|\alpha\beta\rangle$$

$$U(A_-)|\beta\alpha\rangle = i|\beta\beta\rangle$$

$$U(A_-)|\alpha\beta\rangle = i|\alpha\alpha\rangle$$

$$U(A_-)|\beta\beta\rangle = |\beta\alpha\rangle \quad [5]$$

The population of the  $|\alpha\beta\rangle$  state at time point ② is derived from the thermal equilibrium population of the  $|\beta\beta\rangle$  state.

Since the  $|\alpha\beta\rangle$  state is connected adiabatically to the low-field singlet, the sequences  $A_+$  and  $A_-$  may be used to prepare low-field singlet states at time point ③ with populations deviating from the mean in opposite senses.

### Sequence B

The pulse sequence  $B$  is given by  $90_0 - \tau_2 - 180_{90} - \tau_3 - 90_{45}$ , with pulse sequence delays given by  $\tau_2 = |\pi/(2\omega_{\Delta}^{\text{high}})| + |1/(4J)|$  and  $\tau_3 = |1/(4J)|$ . For the experimental results, the delays were set to the values  $\tau_2 = 44.64$  ms and  $\tau_3 = 43.61$  ms. This sequence is designed to separate cleanly the interesting NMR signals deriving from the low-field singlet state from the uninteresting signals generated by relaxation of the spin system during the second transport interval.

From standard spin-operator theory (3,4), the propagator  $U(B)$  for this pulse sequence transforms the population operator of state  $|\alpha\beta\rangle$  into a superposition of many operator terms, including some that represent antiphase single-quantum coherences:

$$\begin{aligned} U(B)I_1^\alpha I_2^\beta U(B)^\dagger = & -\frac{1}{4} \exp\{-i\pi/4\} I_1^- I_2^\alpha - \frac{1}{4} \exp\{+i\pi/4\} I_1^\alpha I_2^- \\ & + \frac{1}{4} \exp\{-i\pi/4\} I_1^- I_2^\beta + \frac{1}{4} \exp\{+i\pi/4\} I_1^\beta I_2^- + \dots \end{aligned}$$

[6]

The  $(-1)$ -quantum coherences represented by operators  $I_1^\alpha I_2^-$  and  $I_1^\beta I_2^-$  generate the diagnostic antiphase signals near the chemical shift  $\delta_2$ .

Sequence  $B$  gives rise to no net signals at the chemical shift  $\delta_2$  when applied to in-phase Zeeman magnetization, created by  $T_1$  relaxation during the second transport interval  $\tau_{\text{transp}}^{(2)}$ . This may be seen from the transformations

$$\begin{aligned} U(B)I_{1z}U(B)^\dagger = & -\frac{1}{2} \exp\{+i\pi/4\} I_1^+ I_2^\alpha - \frac{1}{2} \exp\{-i\pi/4\} I_1^- I_2^\alpha \\ & + \frac{1}{2} \exp\{+i\pi/4\} I_1^+ I_2^\beta + \frac{1}{2} \exp\{-i\pi/4\} I_1^- I_2^\beta \end{aligned}$$

[7]

and

$$U(B)I_{2z}U(B)^\dagger = \frac{1}{2} I_1^+ I_2^+ + i\frac{1}{2} I_1^+ I_2^- - i\frac{1}{2} I_1^- I_2^+ + \frac{1}{2} I_1^- I_2^- \quad [8]$$

Partially-relaxed Zeeman magnetization of spin  $I_1$  only generates signals at the chemical shift  $\delta_1$ , while partially-relaxed Zeeman magnetization of spin  $I_2$  only generates multiple-quantum coherences, which do not generate a signal at all. In principle, cross-correlated relaxation (5) during the transport interval could also generate spurious signals at the shift  $\delta_2$ . Such signals would not change sign when exchanging the sequences  $A_+$  and  $A_-$ , and appear to be negligible in the system studied here.

## Sample

The sample was 500 microlitres of a 17.7 mM solution of 2,3-dibromothiophene in DMSO-d<sup>6</sup>, contained in a 5 mm high-resolution NMR tube equipped with a Young valve to facilitate degassing. The sample contained a water impurity in approximately 27 mM concentration. The sample was subjected to three freeze-pump-thaw degassing cycles, each lasting over 30 minutes, to remove dissolved oxygen.

## Experimental Procedure

The NMR experiments were performed on a Varian Infinity+ 400 MHz NMR system at a field of  $B_{\text{high}} \cong 9.4$  T, using an actively-shielded 89 mm bore magnet. A standard 5 mm high-resolution NMR probe was used. The 90° pulse duration was around 5  $\mu\text{s}$ .

The sample was transported between the high and low fields using the standard pneumatic sample elevator. The air pressure of the elevator was increased during the lift operation, and reduced during the insert operation, in order to accelerate the transport times. With practice we could achieve fairly reproducible transport times of  $\tau_{\text{transp}}^{(1)} = 9 \pm 1$  s and  $\tau_{\text{transp}}^{(2)} = 13 \pm 2$  s, measured from when the sample is fully loaded into the coil to when the sample is outside the magnet bore.

The field  $B_{\text{low}}$  were estimated using a Hall-effect Gauss meter, with zero field calibrated to an accuracy of approximately  $10 \mu\text{T}$  using a mu-metal shield far from the magnet.

For a storage field  $B_{\text{low}} = 20 \text{ mT}$ , the sample was elevated to the top of the magnet bore and allowed to remain there for the time  $\tau_{\text{LP}}$ . For the lower fields, the sample was carried physically to calibrated locations within the stray field of the magnet, or in the case  $B_{\text{low}} = 0$ , into the magnetically-shielded chamber.

### Numerical Simulations

The Liouville-von Neumann equation may be integrated using the low field Liouvillian  $\hat{L}_{\text{LP}}$  (Eq.[8] of the main manuscript) to predict the trajectory of the singlet population as a function of magnetic field and molecular motional parameters.

For 2,3-dibromothiophene, the distance between the proton nuclei was estimated to be  $r = 253 \text{ pm}$ . The spin-lattice relaxation in high field was assumed to be dominated by intramolecular dipole-dipole relaxation, modelled as the isotropic rotational diffusion of a rigid molecule. With this model, the observed  $T_1$  value of  $20 \text{ s}$  corresponds to a rotational correlation time of  $\tau_a = 15 \text{ ps}$ .

Dynamic simulations of the singlet state population as a function of time and field are shown in Fig.1. At low values of the field  $B_{\text{low}}$ , the singlet state

Fig.1

population is predicted to be time-independent over a timescale of hundreds of seconds. As the storage field is increased beyond around 200 mT, a rapid low-amplitude oscillation of the singlet state population is superimposed on a slower decay. At higher fields the amplitude of the oscillations becomes very large and at long times the population equilibrates among the four available states, indicating the loss of all spin order.

The experimental results show a significant damping of singlet spin order on the timescale of 100 seconds for fields much less than 200 mT. This indicates the participation of relaxation mechanisms other than intramolecular dipole-dipole coupling. Intermolecular dipole-dipole relaxation involving water protons or protons on different DBT molecules is likely to be the major singlet damping mechanism.

## References.

1. M. H. Levitt, *J. Magn. Reson.* 126, 164 (1997).
2. M. H. Levitt and O. G. Johannessen, *J. Magn. Reson.* 142, 190 (2000).
3. R. R. Ernst, G. Bodenhausen and A. Wokaun, *Principles of Nuclear Magnetic Resonance in One and Two Dimensions* (Clarendon Press, Oxford, UK, 1987).
4. M. H. Levitt, *Spin Dynamics. Basics of Nuclear Magnetic Resonance* (Wiley, Chichester, UK, 2001).
5. Anil Kumar, R. Christy Rani Grace and P. K. Madhu, *Prog. NMR Spectrosc.* 37, 191 (2000).

## Figure Captions.

Fig.1. Simulated trajectories of the singlet state population for the case  $\delta_1 = 7.11$  ppm,  $\delta_2 = 7.72$  ppm,  $J = 5.7$  Hz,  $r = 253$  pm and  $\tau_c = 15$  ps. The values of  $B_{low}$  are shown in the figure. The population of the singlet state is tracked starting from an initial condition in which the singlet is 100% populated and all the other states have zero population. At high storage fields, the singlet state population is predicted to oscillate rapidly and decay towards a final value of 25%, representing an equal distribution of populations amongst the four states. The dark areas indicate very rapid oscillations of the singlet population.

**This Page is Inserted by IFW Indexing and Scanning  
Operations and is not part of the Official Record**

## **BEST AVAILABLE IMAGES**

Defective images within this document are accurate representations of the original documents submitted by the applicant.

Defects in the images include but are not limited to the items checked:

- BLACK BORDERS**
- IMAGE CUT OFF AT TOP, BOTTOM OR SIDES**
- FADED TEXT OR DRAWING**
- BLURRED OR ILLEGIBLE TEXT OR DRAWING**
- SKEWED/SLANTED IMAGES**
- COLOR OR BLACK AND WHITE PHOTOGRAPHS**
- GRAY SCALE DOCUMENTS**
- LINES OR MARKS ON ORIGINAL DOCUMENT**
- REFERENCE(S) OR EXHIBIT(S) SUBMITTED ARE POOR QUALITY**
- OTHER:** \_\_\_\_\_

**IMAGES ARE BEST AVAILABLE COPY.**

**As rescanning these documents will not correct the image problems checked, please do not report these problems to the IFW Image Problem Mailbox.**